Revista Mexicana de Astronomía y Astrofísica, **44**, 213–220 (2008)

CHEMICAL COMPOSITION IN FAST ROTATORS MAIN SEQUENCE STARS

C. R. Fierro and L. Georgiev

Instituto de Astronomía
Universidad Nacional Autónoma de México, Mexico

Received 2007 July 23; accepted 2008 February 6

RESUMEN

Usando datos públicos del Ultraviolet and Visual Echelle Spectrograph Paranal Observatory Project (UVES POP), y con el método de la transformada de Fourier, se obtuvieron las velocidades de rotación proyectadas, $v \sin i$, para 16 estrellas en el campo del cúmulo galáctico IC 2391 (o Vel Cluster). Se encontró que sólo 12 de dichos objetos son miembros del cúmulo y al separarlos en dos grupos (estrellas de secuencia principal y estrellas evolucionadas) se encontró una correlación entre la velocidad de rotación y la temperatura efectiva, lo que indica que las estrellas dentro del cúmulo tienen aproximadamente la misma orientación del eje de rotación. Los cocientes N/C y O/C obtenidos para las estrellas de secuencia principal se incrementan con $v \sin i$, mostrando evidencias de mezclado inducido por rotación.

ABSTRACT

Using public data of the Ultraviolet and Visual Echelle Spectrograph Paranal Observatory Project (UVES POP) the projected rotational velocities, $v \sin i$, for 16 stars in the field of the galactic cluster IC 2391 (o Vel Cluster) were obtained using the method of the Fourier transform (FT). We found that only 12 of these objects are cluster members and separating them in two sets (main sequence stars and evolved stars) a correlation of the rotation velocity with the effective temperature was found, indicating a nearly equal orientation of the rotation axis for the member stars. The ratios N/C and O/C obtained for the main sequence stars increase with $v \sin i$ and show evidence of mixing induced by rotation.

Key Words: stars: early-type — stars: abundances — stars: rotation

1. INTRODUCTION

Models for rotating stars with intermediate and high masses ($2\ M_\odot \leq M \leq 60\ M_\odot$) predict that the chemical composition in stellar atmospheres is changed because the rotation favors the mixing of the material in the atmosphere with that processed in the stellar core through the CNO cycle (Zahn 1992; Meynet & Maeder 1997). Due to this an increase of the ratios N/C and N/O is expected in the stellar photosphere at the end of the main sequence (MS) phase (Meynet & Maeder 2000, 2002). The surface enrichments on the main sequence generally depend on the following factors: the initial mass, the initial metallicity, the initial rotational velocity and the age of the star. The mixing is more efficient in massive stars with lower initial metallicities and large rotational velocities (Meynet & Maeder 2000). The ratio N/O is a good test for the origin of nitrogen. When N is primary, N/O is expected to be approximately constant, since nitrogen results from the procesed oxygen by the CNO cycle during hydrogen burning. In this context, the study of the stars within a cluster allows one to assume the same age and chemical composition for all the stars; then the observed changes in abundances can be related to the mass and initial rotational velocities only. A good tool for determining the stellar parameters are the synthetic spectra generated by codes such as ATLAS9 (Kurucz 1970) and ATLAS12 (Kurucz 2005), which allow us to obtain the effective temperature ($T_{\rm eff}$), the gravity and the chemical abundances.

Diverse techniques are used to obtain the projected rotational velocity v sin i. The one mostly used consists in comparing the spectral lines of a star with those of standard stars such as the old system of Slettebak (1949, 1954, 1955, 1956), and more recently the new system of Slettebak (1979). Another very popular method consist in generating a synthetic profile for a specific spectral line and finding the best fit for the observed one (Korn et al. 2005). On the other hand, Carroll (1933) was the first to use the method of the Fourier transform (FT) for obtaining v sin i. Nevertheless, due to the low quality of the data then available, the uncertainties were large. Gray (1976) described a method for obtaining v sin i, using the first zero of the FT. This technique is more precise, and with good quality data the uncertainties were reduced. In this paper we use the FT technique and high resolution echelle spectra in order to derive rotational velocities with good precision.

The aim of this work is to study the abundances of C, N, and O in stars of the galactic cluster IC 2391 searching for evidence of a stellar material mixing induced by rotation, i.e. a positive correlation between log N/C and the rotational velocity. In addition, we investigate the behavior with v sin i of the distinct stellar parameters: $T_{\rm eff}$, log g, mass. In § 2 we describe the stellar spectra used in this study. In § 3 the method used for measuring v sin i is presented . In § 4 we discuss the criteria used to discriminate between cluster members and field stars. § 5 describes the methods for obtaining the stellar parameters: effective temperature ($T_{\rm eff}$), logarithm of the gravity (log g), and C, N, O abundances. In § 6 the results are discussed, and finally the conclusions are given in § 7.

2. THE STELLAR SPECTRA

This work is based on the data obtained from the Ultraviolet and Visual Echelle Spectrograph Paranal Observatory Project (UVES POP) produced for public use under ESO Director Discretionary Time (DDT) Program 266.D-5655(A) (Bagnulo et al. 2003). The available spectra are of high quality, with S/N $\geq$ 400–500 in the V band and spectral resolution ∼80000. The Balmer jump allows us to estimate $T_{\rm eff}$. On the other hand the quality of weak lines in these spectra is good until $\lambda \approx 5820$ Å. For this reasons we chose to use the data available in the 3600 Å$\leq$ λ $\leq$ 6000 Å range. We analysed all stars earlier than A5. These stars have higher cluster membership probability and higher expected v sin i.

3. THE v sin i MEASUREMENT

The observed profile of a spectral line in a rotating star $F(\lambda)$, can be written as the convolution of the instrumental profile $I(\lambda)$, intrinsic profile $H(\lambda)$ and rotational profile $G(\lambda)$:

$$F(\lambda) = I(\lambda)H(\lambda)G(\lambda) \quad ; \qquad (1)$$

shifting to the frequency domain, we obtain the FT:

$$f(\nu) = i(\nu)h(\nu)g(\nu) \quad , \qquad (2)$$

where $f(\nu)$, $i(\nu)$, $h(\nu)$, $g(\nu)$ are the FTs from $F(\lambda)$, $I(\lambda)$, $H(\lambda)$, $G(\lambda)$ respectively. The main problem is to obtain $g(\nu)$ with an adequate S/N. There are many techniques for this. Some works use a method introduced by Gray (1976) obtaining $g(\nu)$ from:

$$g(\nu) = \frac{f(\nu)}{i(\nu)h(\nu)} \quad , \qquad (3)$$

and comparing to the FT of a theoretical rotation profile generated ad hoc, fitting the position of the first zero (ν_0). The division in (3) enhanced the noise at higher frequencies. This can be improved by multiplying the FT by a Bessel weighting function and integrating over Fourier frequency. A simpler method suggested also by Gray (1976) is to compute a theoretical profile for v sin i=1 km s^{-1}, then ν_0 for this profile is compared with the first zero of g(ν) from a spectral line ($\nu_{0\lambda}$) and the rotational velocity is derived from

$$v \sin i = \frac{\nu_0}{\nu_{0\lambda}} \quad . \qquad (4)$$

This is straightforward. However, there remains the problem of obtaining $g(\nu)$ with good resolution and S/N. With the resolution of the available data $I(\lambda) \leq G(\lambda)$. When the width of a signal in the time domain is large, the FT is narrow and vice versa, therefore, $i(\nu)$ and $h(\nu)$ are broad while $g(\nu)$ is narrow and is less affected by the $i(\nu)$ and $h(\nu)$ profiles. We can then assume $f(\nu) \sim g(\nu)$.

The resolution theorem expreses that only the frequencies $\nu < W$, where W is the width of the data window, can be recorded in the FT while the high frequency components of the signal are missing. A sharp feature in $f(\nu)$ of size $\delta\nu$ can be resolved by extending the bandwidth W, requiring

$$\Delta\nu \leq \frac{1}{W} \quad . \qquad (5)$$

In this context we isolated the Mg II λ4481 line and added points in the continuum at both sides of

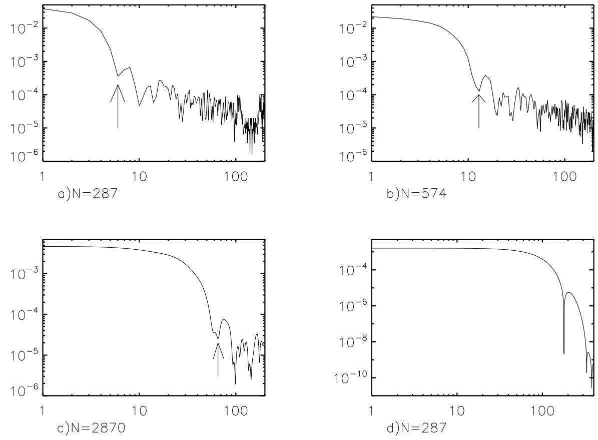

Fig. 1. (a), (b) and (c) show the FT for Mg II λ4481 line of HD 74146. The resolution of the FT improves by adding points in the continuum. When N is the number of the points in the data window, althoug the value of the $\nu_{0\lambda}$ changes the rate $\nu_{0\lambda}$/N, remains constant; (a) $\nu_{0\lambda}$= 6.027, $\nu_{0\lambda}$/N=0.021; (b) $\nu_{0\lambda}$=12.99, $\nu_{0\lambda}$/N=0.023; (c) $\nu_{0\lambda}$=65.335, $\nu_{0\lambda}$/N=0.023. Note that the value of $\nu_{0\lambda}$ is poorly defined in (a) while in (c) is easy to measure; (d) shows the FT of the theoretical profile with v sin i=1 km s^{-1}, ν_0=178.462, ν_0/N=0.622. Using the equation (4) we obtained v sin i=27 km s^{-1} for the profile show in (c).

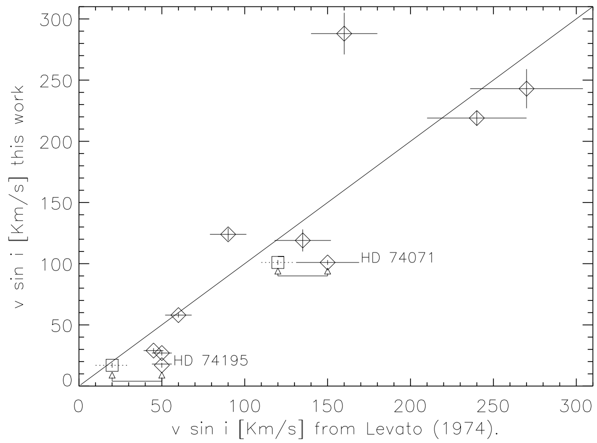

Fig. 2. Comparision between v sin i obtained in this study with other authors. Diamonds represent v sin i derived in this work compared to the values from Levato (1974). Two objects: HD 74071 and HD 74195 have a second value of v sin i from Levato & Malaroda (1970) represented by squares. The rotational velocities of these two stars were derived with the same method in both works but the spectra were obtained with different telescopes (see the text). The solid line stands for the one-to-one relation.

the line, obtaining a better resolution in the determination of the first zero in the FT. If N is the number of points in the data window when N increases the value of the first minimum in the FT changes, but the rate $\nu_{0\lambda}/N$ is roughly constant independently of the value of N (Figure 1). The line most frequently used in the v sin i determination is Mg II λ4481, because it is relatively isolated, not very sensitive to effective temperature ($T_{\rm eff}$) and gravity changes, and is strong in Type A and B stars; therefore it is observable even in fast rotators.

The Mg II λ4481 line is really a triplet (4481.126 + 4481.150 + 4481.325). In order to study the effect of taking three lines instead one in the FT we generated a synthetic spectrum using the ATLAS12 code (Kurucz 2005). Subsecuently, with the SYNTHE code (Kurucz 1970) this spectrum was rotated in the range of 2 km s^{-1} to 30 km s^{-1} with steps of 2 km s^{-1} and with a resolution similar to that of the observed spectra. In these models it was found that the spectral resolution does not allow velocities less than 18 km s^{-1}. This is the lower limit in our measurements and for rotational velocities greater than this value the triplet of Mg II $\lambda\lambda\lambda$4481.126, 4481.150, 4481.325 behaves as a single line, and does not have any effect on the first minimun of the FT value. The errors were computed from the difference in the values of v sin i obtained from the lines of Mg II λ4481 and He I λ4471. In general, the errors are less than 10% of v sin i. When the error was less than the instrumental width we assumed an error of 2 km s^{-1}.

The projected rotational velocities, v sin i, were obtained for 12 type B and 4 type A stars in the galactic cluster IC 2931 (Table 1). We compare the results with the data obtained by other authors (Uesugi & Fukuda 1982, Revised Catalogue of Stellar Velocities). This catalogue is a compilation from several sources. The majority of the v sin i values common with this study came from the work of Levato (1974). Figure 2 shows the comparision of the projected rotational velocities obtained from this work versus those obtained from Levato with observations made at the 91 cm reflector of Cerro Tololo Inter-American Observatory in 1974, in which the minimum detectable rotational velocity is about 45 km s^{-1}. The values of v sin i for HD 74071 and HD 74195 from Levato & Malaroda (1970) were also plotted. Figure 2 shows a good correlation. The cut at v sin i = 45 km s^{-1} in the data from Levato (1974) is noticeable.

4. CLUSTER MEMBER SELECTION

The obtained data are shown in Table 1. The data in Columns 1, 2, 3, 4, and 5 were obtained from the UVES Paranal Observatory Project web-

TABLE 1

STELLAR PARAMETERS

Star	Sp. Type	V	$B-V$	$U-B$	E_{B-V}	$V-M_V$	$T_{\rm eff}$	M_{bol}	$v \sin i$ This work	$v \sin i$ Levato	Cluster Member
HD 73287	B7V	7.070	−0.110	−0.460	0.029	7.107	14100	−0.220	182±2		no
HD 73503	A0V	8.350	0.040	−0.110	0.100	6.936	10200	0.657	123±7		yes
HD 73681	A1V	7.860	0.086	0.023	0.296	5.915	8800	0.757	119±9	135	yes
HD 73952	B9Vn	6.460	−0.100	−0.330	0.000	5.949	11850	−0.216	219±6	240	yes
HD 74071	B5 V	5.472	−0.160	−0.563	0.002	5.704	14950	−1.555	101±2	120[d]	yes
HD 74146	B4IV	5.180	−0.140	−0.576	0.031	5.593	14300	−1.972	27±2	50	yes
HD 74168	B9 p	7.510	−0.120	−0.470	0.020	7.355	11650	−1.009	71±5		yes
HD 74195	B3IV	3.610	−0.180	−0.640	0.003	5.906	15950	−3.850	18[c]	20[d]	yes
HD 74196	B7Vn	5.610	−0.140	−0.500	0.005	5.803	13900	−1.359	288±17	160	yes
HD 74275	A0V	7.290	−0.008	−0.043	0.013	5.750	10200	1.522	58±2	60	no
HD 74516	A5V	7.390	0.020	0.010	0.060	5.945	9600	1.502	124±5	90	yes
HD 74535	B8s	5.510	−0.148	−0.556	0.014	5.853	11850	−1.711	35±5		yes
HD 74560	B3IV	4.841	−0.170	−0.665	0.022	5.837	16150	−2.736	29±2	≤45	yes
HD 75067	B9IV[a]	9.430	−0.010	−0.280	0.091	5.750	12900	2.881	320±3		no
HD 75105	B8III[b]	7.670	−0.090	−0.475	0.060	5.750	12700	0.801	122±3		no
HD 75466	B8V	6.275	−0.100	−0.315	0.000	5.768	11600	−0.181	243±16	270	yes

[a]Spectral Type is doubtful whether B8Vn and B9IV.
[b]Spectral Type is doubtful whether B8III and B8IV.
[c]This value correspond with the inferior limit measurable in this work, the actual v sin i maybe smaller.
[d]Values from Levato & Malaroda (1970).

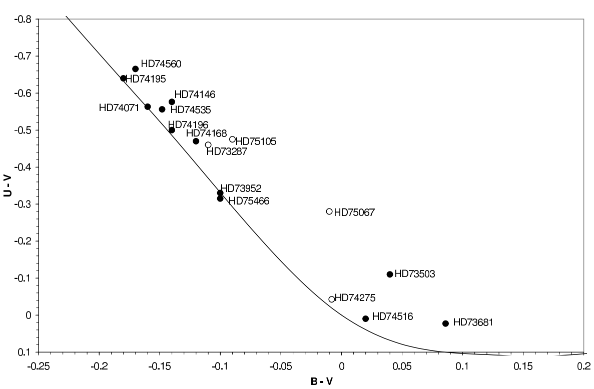

Fig. 3. Color-color diagram. Filled circles represent the cluster members. Open circles are the objects discarded as members of the cluster. Note that with exception of HD 74275 these are reddened stars. The solid line is the position of the ZAMS.

page. We obtained $E_{(B-V)}$ for each star using the color magnitude diagram (Figure 3), and assuming R=3.2. The results are presented in Column 6 of Table 1. The distance moduli in Column 7 were obtained from the parallaxes of *Hipparcos.* The average distance to the cluster calculated from the available parallaxes is $\sim$ 163 pc. This distance was assigned to the stars with unknown parallax. The $T_{\rm eff}$, presented in Column 8, was obtained from the synthetic spectra generated with the codes ATLAS12 and SYNTHE, while $M_{\rm bol}$, presented in Column 9, was calculated using the equations of Table IX in Massey, Parker, & Garmany (1989). Figure 4 shows the H-R diagram for the analysed objects. In order to determine the evolving status of the objects the evolutionary tracks for solar metallicity from Lejeune & Schaerer (2001) were overplotted on the H-R diagram (Figure 4). Comparing Figures 3 and 4 we assumed that the cluster members are those with small reddening (e.g. HD 74195, HD 74071, HD 74168) in the region covered by the evolutionary tracks. HD 73287 and HD 74275 lie outside this region. For the first star the parallax indicates a distance of 116 pc, larger than the average distance to the cluster, while the parallax of the second star is unknown. HD 75067 and HD 75105 are more reddened stars and also lie outside the region covered by the evolutionary tracks. The parallax of the second star indicates a distance of 136 pc, larger than the average distance, while the parallax of the first star is unknown. For these reasons the four objects: HD 73287, HD 74275, HD 75067 and HD 75105 were discarded as cluster members.

5. DETERMINATION OF STELLAR PARAMETERS

Synthetic spectra were generated by the codes ATLAS12 and SYNTHE adapted for running under the GNU Linux plataform (Sbordone et al. 2004; Sbordone 2005; Castelli 2005). We made a grid of models covering the ranges 10000 K $\leq T_{\rm eff} \leq$ 17000 K, with steps of 1000 K and 3.1 $\leq \log g \leq$ 4.7 with steps of 0.4 dex.

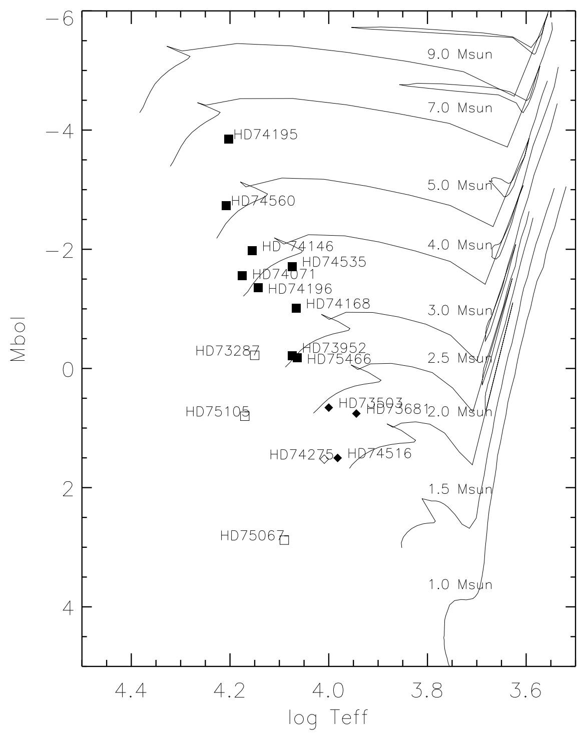

Fig. 4. H-R diagram of the analysed stars. The evolutive tracks correspond to solar metallicity Z=0.02 (Lejeune & Schaerer 2001). Filled circles are type B stars cluster members, open circles are type B field stars, fill triangles type A stars in cluster and open triangles type A field stars. Note that in general no cluster members stand out of the evolutive tracks.

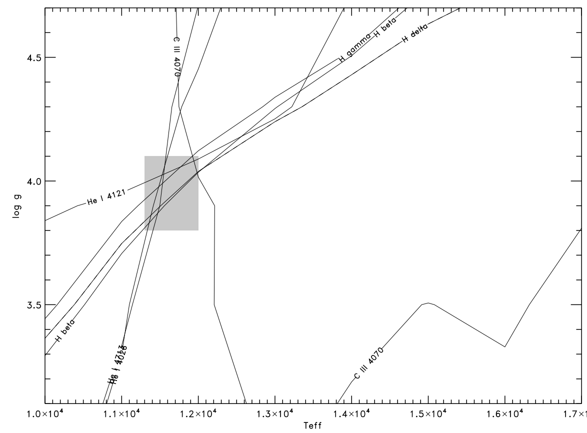

Fig. 5. Determination of temperature and gravity by means of isocontour plot for HD74168. All the lines are crossed in the filled area allow us to obtain effective temperature 11650±350 K and log g=3.95±0.15.

The Balmer lines are very sensitive to the gravity and they are broadened when log g increases. Thus, the widths of these lines measured at a certain depth are a good indicator of log g. We measured the width of H_β, H_γ and H_δ at a depth=0.75 in the normalized spectra, in both the models and the stellar spectra. In addition, the equivalent widths (EW) of lines sensitive to $T_{\rm eff}$ such as Ca I λ4226, Ca II λ3949, Fe II λ4179 and λ4233 were measured for type A stars. The lines He I λ4026, λ4121, λ4713, Si II λ4552, C III blended with O II λ4070 were chosen for type B stars. With the obtained values from the stellar spectra we constructed isocontour plots. $T_{\rm eff}$ and gravity were determined from the crossing region of the isocontours. Figure 5 shows an example of these graphs.

The next step was to compute synthetic spectra with $T_{\rm eff}$, log g and v sin i as obtained, but changing the abundances in a range from 0.1 to 10 times the solar value for each element. In each set of models we looked for the lines sensitive to abundance changes. The number of these lines decreases with the rotation, since in fast rotators the lines are blended. The EWs of these lines were measured in both the models and the stellar spectra in order to construct curves of growth for each element C, N and O for which the abundance was measured. The values listed in Table 2 are the averages of all the lines available in each spectra. The errors were computed from the differences in these values. Synthetic spectra were generated with the stellar parameters: $T_{\rm eff}$, log g, log C, log N, log O and v sin i obtained with the methods described above. These spectra were compared with the observed ones, finding a good agreement. Figure 6 shows an example of the fit between the synthetic and observed spectrum for HD 73503.

6. RESULTS AND DISCUSSION

The assumption usually made is that the axes of rotation are randomly distributed in space. This hypothesis has been tested by Gaigé (1993) for the following open clusters: α Persei, the Hyades, the Pleiades, Praesepe and Coma Berenice. It was found likely to be correct.

Abt, Levato, & Grosso (2002) in their study of 451 nothern B8-B9.5 III, IV and V stars found a bimodal distribution of v sin i and concluded that the slow rotators are Ap stars which often evolve to the upper edge of the main sequence. Therefore their luminosity classes are III or IV, while the rapid rotators are normal B stars with luminosity classes III, IV and V.

In this work members of the cluster IC 2391 are separated in two sets: main sequence and subgiant stars. In order to classify the objects as

TABLE 2

MAIN SEQUENCE STARS

Star	$T_{\rm eff}$	log g	$M/M_\odot$	v sin i	log C	log N	log O	log N/C	log O/C	log N/O
HD73681	8800 ± 350	4.25 ± 0.30	2.61	119 ± 9	-3.59 ± 0.35	-4.28 ± 0.28	-3.36 ± 0.27	-0.69 ± 0.63	0.23 ± 0.55	-0.92 ± 0.55
HD73503	10200 ± 200	4.45 ± 0.40	2.24	123 ± 2	-3.52 ± 0.39	-4.37 ± 0.24	-2.82 ± 0.26	-0.85 ± 0.63	0.70 ± 0.65	-1.55 ± 0.05
HD74516	9600 ± 400	4.45 ± 0.25	2.43	124 ± 5	-3.25 ± 0.23	-4.31 ± 0.20	-3.00 ± 0.20	-1.06 ± 0.43	0.25 ± 0.40	-1.31 ± 0.40
HD73952	11850 ± 350	4.05 ± 0.15	3.31	219 ± 6	-3.67 ± 0.23	-4.10 ± 0.20	-3.03 ± 0.20	-0.43 ± 0.43	0.64 ± 0.40	-1.07 ± 0.40
HD75466	11600 ± 400	4.28 ± 0.30	3.28	243 ± 16	-4.12 ± 0.20	-4.35 ± 0.20	-3.08 ± 0.20	-0.23 ± 0.40	1.04 ± 0.60	-1.27 ± 0.40
HD74196	13900 ± 500	4.25 ± 0.30	4.36	288 ± 17	-3.68 ± 0.20	-4.10 ± 0.20	-3.00 ± 0.20	-0.42 ± 0.40	0.68 ± 0.40	-1.1 ± 0.40
HD74071	14950 ± 350	4.15 ± 0.15	4.58	101 ± 2	-3.78 ± 0.20	-3.40 ± 0.20	-3.47 ± 0.20	0.38 ± 0.40	0.31 ± 0.40	0.07 ± 0.40

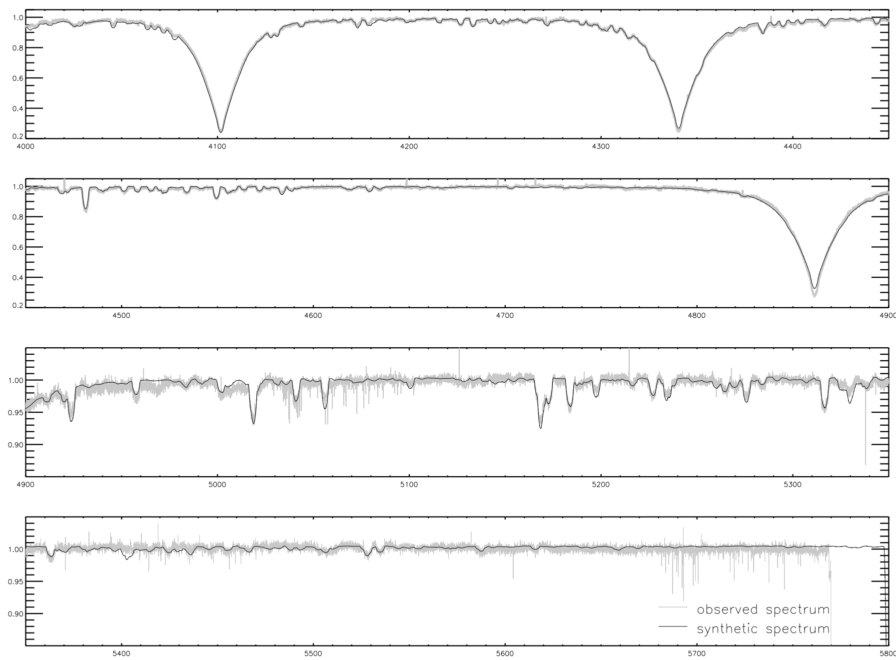

Fig. 6. Comparision of the synthetic with the observed spectrum for HD 73503 show a good fit. The synthetic spectra was obtained with v sin i=123 km s^{-1}, $T_{\rm eff}$=11200 K, log g=4.45, log C=-3.52, log N=-4.37 and log O=-2.82.

main sequence or evolved stars we take into account their position on the evolutionary tracks in the H-R diagram, their spectral type and the ratios Si III λ4552/He I λ4387, He I $\lambda\lambda$4144/4121 and He I λ4471/Mg II λ4481 used as luminosity criteria (Walborn & Fitzpatrick 1990). We found that the MS stars are all fast rotators with 100 km s^{-1} $\leq v$ sin i $\leq$ 300 km s^{-1} (Table 2), independently of whether they are A or B type, while the evolved stars are slow rotators with v sin $i \leq 50$ km s^{-1} (Table 1).

In the chemical composition analysis it was found that HD 74071 is rich in nitrogen. Except for this object the plot of effective temperature vs rotational velocity (Figure 7) shows a correlation of these parameters for the MS stars, in the sense that v sin i increases with $T_{\rm eff}$. This behavior is consistent with angular momentum conservation. The hotter, more massive, stars are formed from a larger cloud; therefore, after contraction, they should have rotational velocities greater than those of the cooler, less massive, stars. When the star leaves the MS, its atmosphere is expanded and the rotational velocity is reduced. The best fit of this correlation was the line:

$$T_{\rm eff} = 23.76\ v \text{ sin } i\ [\text{km s}^{-1}]\, K + 6571.73\ K \quad , \quad (6)$$

with a correlation index 0.95.

Since 6 of the 7 main sequence stars fall on this line, we can infer that the direction of the rotation axis is approximately the same for the main sequence stars within the cluster.The discrepancy with the assumption of the stellar axes being randomly oriented can be explained by the fact that other studies do not make a separation of the objects according to the evolutionary stage.

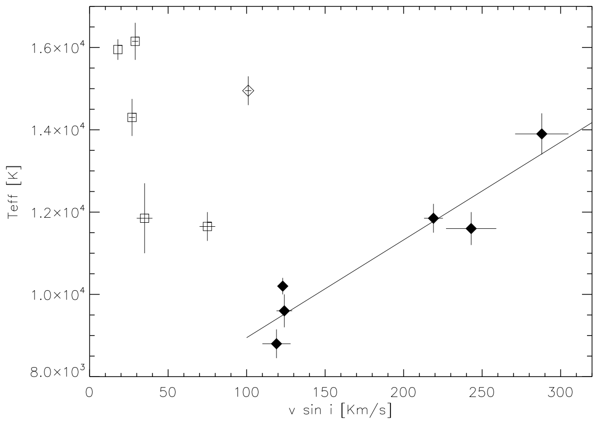

Fig. 7. $T_{\rm eff}$ versus v sin i. Open squares are the evolved stars. Filled diamonds are the main sequence stars wich show correlation of the effective temperature with rotational velocities. The solid line is the best adjustment of the data. The open diamond represents HD 74071, a main sequence star with enhanced N.

Table 2 shows the chemical composition obtained for the seven stars on the main sequence. The errors were estimated from the dispersion in the values obtained for different lines of the same element. The spectroscopic masses in Column 4 were obtained from M_V and the mass-luminosity relation of Kroupa & Gilmore (1993), showing a good agreement with the masses inferred from the evolutive tracks in the H-R diagram. Figure 8 shows the behavior of log N/C, log O/C and log N/O with rotation. With the exception of HD 74071, represented with an open circle, this figure shows that log N/C increases with rotation, following a linear tendency. In the same way it is observed that log O/C also increases with rotation. The nearly constant behavior of log N/O indicates that the N excess has a primary origin. This result cleary indicates that when rotation increases, the amount of carbon at the stellar surface decreases, whereas nitrogen and oxygen increase. Theoretical models of massive and intermediate-mass stars with initial rotational velocities of 300 km s^{-1} predict depletion of C and O, with N enhanced at the end of the MS (Talon et al. 1997; Meynet 2000; Maeder & Meynet 2000; Meynet & Maeder, 2000). In this context, our results show that rotation favors surface enrichments with processed material of the CNO cycle. In Table 2 and Figure 8 it is noticeable that HD 74071 is a nitrogen rich star. Its value of log O/C shows a behavior similar to the other objects, while log N/C and log N/O are higher for this star than for the others in the sample. During the helium burning phase, intermediate mass stars may evolve from the red giant branch (RGB) to the blue giant region and return. This phenomenon was first found by Hayashi, Hoshi, & Sugimoto (1962) and is called the blue loop. HD 74071 could be an object that experimented this blue loop, changing its chemical composition.

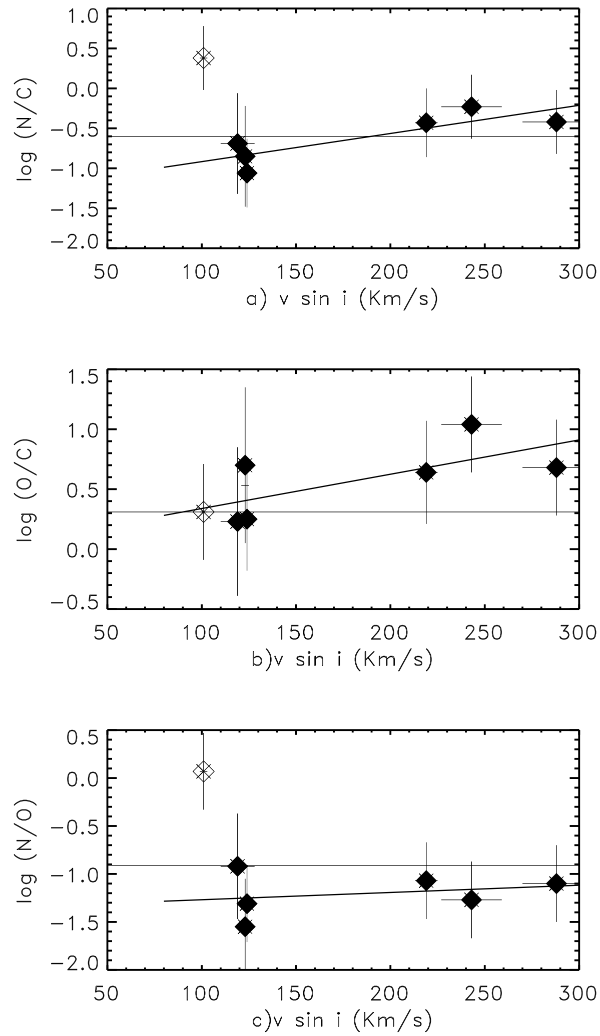

Fig. 8. (a) log N/C, (b) log O/C, (c) log N/O vs v sin i. Note that HD 74071 (open diamond) has a nitrogen excess. The normal main sequence stars show a positive correlation of log N/C with the rotation, log N/C also increases with v sin i too, while that log N/O is nearly constant indicating primary nitrogen.

7. CONCLUSIONS

Using the method of the Fourier transform we have obtained rotational velocities for early stars in the field of the galactic cluster IC 2391. The fast rotators are MS stars, while the slow rotators correspond to evolved stars. For the MS cluster members we obtained a correlation between $T_{\rm eff}$ and v sin i, finding that the hotter MS stars have high rotation. The results obtained indicate that the orientation of the rotation axes is still the same for the main sequence stars of the same cluster. When studying the chemical abundances of MS stars we found that, within the error bars, log N/C and log O/C increase with rotation, while log N/O is constant, thus corroborating the theoretical predictions of mixing of stellar material induced by rotation.

We express our deep thanks to Fiorella Castelli for her help to generate synthetic spectra with ATLAS12 and SYNTHE under Linux, to the UVES Paranal Observatory Project for the access to the data on wich this investigation is based, to Jana Benda for her revision of this paper and to Alfredo Diaz for his computational support.

REFERENCES

Abt, H., Levato, H., & Grosso, M. 2002, ApJ, 573, 359
Bagnulo, S., Jehin, E., Ledoux, C., Cabanac, R., Melo, C., & Gilmozzi, R. 2003, ESO Messenger, 114, 10
Carroll, J. A. 1933, MNRAS, 93, 478
Castelli, F. 2005, Mem. Soc. Astron. Italiana Suppl., 8, 25
Gaigé, Y. 1993, A&A, 269, 267
Gray, D. F. 1976, The Observation and Analysis of Stellar Photospheres (New York: Wiley)
Hayashi, C., Hoshi, R., & Sugimoto, D. 1962, Prog. Theor. Phys. Suppl., 22, 1
Kroupa, I., & Gilmore, G. 1993, MNRAS, 262, 545
Korn, A. J., Nieva, M. F., Daflon, S., & Cunha, K. 2005, ApJ, 633, 899
Kurucz, R. L. 1970, SAO Spec. Rep., 309, 291
__________. 2005, Mem. Soc. Astron. Italiana Suppl., 8, 14
Levato, H. 1974, PASP, 86, 940
Levato, H., & Malaroda, S. 1970, PASP, 82, 741
Lejeune, T., & Schaerer, D. 2001, A&A, 366, 538
Maeder, A., & Meynet, G. 2000, ARA&A, 38, 143
Massey, P., Parker, J. W., & Garmany, C. D. 1989, AJ, 98, 1305
Meynet, G. 2000, in ASP Conf. Ser. 198, Stellar Clusters and Associations: Convection, Rotation, and Dynamos, ed. R. Pallavicini, G. Micela, & S. Sciortino (San Francisco: ASP), 3
Meynet, G., & Maeder, A. 1997, A&A, 321, 465
__________. 2000, A&A, 361, 101
__________. 2002, A&A, 390, 561
Sbordone, L. 2005, Mem. Soc. Astron. Italiana Suppl., 8, 61
Sbordone, L., Bonifacio, P., Castelli, F., & Kurucz, R. L. 2004, Mem. Soc. Astron. Italiana Suppl., 5, 93
Slettebak, A. 1949, ApJ, 110, 498
__________. 1954, ApJ, 119, 146
__________. 1955, ApJ, 121, 653
__________. 1956, ApJ, 124, 173
__________. 1979, Space Sci. Rev., 23, 541
Talon, S., Zahn, J. P., Maeder, A., & Meynet, P. 1997, A&A, 322, 209
Uesugi, A., & Fukuda, I., 1982, Revised Catalogue of Stellar Rotational Velocities (Kyoto: Univ. Kyoto)
Walborn, N., & Fitzpatrick, E. 1990, PASP, 102, 379
Zahn, J. P. 1992, A&A, 265, 115

Celia Rosa Fierro Santillán and Leonid N. Georgiev: Instituto de Astronomía, Universidad Nacional Autónoma de México, Apdo. Postal 70-264, 04510 México, D. F., Mexico (crfierro, georgiev@astroscu.unam.mx).